

## A Dynamical Description of Fall and Winter Mean Current Profiles over the Northern California Shelf\*

STEVE LENTZ AND JOHN TROWBRIDGE

*Woods Hole Oceanographic Institution, Woods Hole, Massachusetts*

(Manuscript received 4 August 1999, in final form 15 June 2000)

### ABSTRACT

Fall and winter mean current profiles from a midshelf (water depth  $\sim 90$  m) northern California site exhibit a similar vertical structure for several different years. The alongshelf flow is poleward with a maximum velocity of  $5\text{--}10\text{ cm s}^{-1}$  in the middle or upper water column. There is an offshore flow of about  $2\text{ cm s}^{-1}$  in the upper  $20\text{--}30$  m, an onshore flow of about  $2\text{ cm s}^{-1}$  in the interior (depths  $35\text{--}65$  m), and an offshore flow of about  $1\text{ cm s}^{-1}$  within  $20$  m of the bottom. Profiles are similar for averages over timescales from weeks to months. Mean current profiles at other midshelf sites along northern California and two sites off Peru also have a similar vertical structure.

The vertical shear in the mean alongshelf flow is geostrophic throughout the water column, that is, in thermal wind balance with the cross-shelf density gradient. For timescales of a week or longer the thermal wind balance extends to within  $1$  m of the bottom and reduces the mean near-bottom alongshelf flow to  $1\text{ cm s}^{-1}$  or less. These observations support recent theoretical work suggesting that, over a sloping bottom, adjustment of the flow and density fields within the bottom boundary layer may reduce the bottom stress. The alongshelf momentum balance is less clear. Weekly averages of offshore transports in the upper and lower water column, relative to the interior onshore flow, are correlated with the surface and bottom stresses, suggesting Ekman balances. However, both the surface and bottom stresses are generally too small by a factor of  $2\text{--}3$  to account for the offshore transports. Limited data suggest that alongshelf buoyancy gradients, estimated over scales of  $15\text{ km}$  or less, can be a significant component of the alongshelf momentum balance within both the upper and lower water column.

### 1. Introduction

The characteristics and dynamics of continental shelf circulations on timescales of months or longer are not well understood. Along the west coast of the United States from Point Conception, California, to Washington existing data indicate a poleward, alongshelf mean flow of  $5\text{--}10\text{ cm s}^{-1}$  during the fall and winter (Strub et al. 1987; Largier et al. 1993). This poleward mean flow is thought to be driven by an alongshelf pressure gradient (Hickey and Pola 1983; Largier et al. 1993) since mean wind stresses tend to be weak and, in the southern part of this domain, equatorward, that is, in the opposite direction. Little is known about the vertical structure, interannual variations, or the dynamics of this mean flow because there are so few long time series of currents.

Until recently, much of our theoretical intuition re-

garding steady shelf circulation has been based on the Arrested Topographic Wave model of Csanady (1978). This is a depth-averaged, frictional model of the shelf circulation that assumes bottom stress is proportional to the depth-averaged flow. Recent theoretical studies suggest that the response of a stratified flow over a sloping bottom may be quite different from the Arrested Topographic Wave response because adjustment of the flow and density fields within the bottom boundary layer may reduce or even eliminate the bottom stress acting on low-frequency flows (Garrett et al. 1993; Middleton and Ramsden 1996; Chapman and Lentz 1997). However, observational evidence either supporting or refuting this type of response in the ocean is limited (Lentz and Trowbridge 1991; Trowbridge and Lentz 1998; Stahr and Sanford 1999).

Midshelf moored current observations from a sequence of field programs on the northern California shelf between 1981 and 1991 provide an opportunity to characterize both the vertical structure and interannual variability of the fall and winter mean flow. Current observations from the Shelf Mixed Layer Experiment (SMILE) and the Sediment Transport Events on Shelves and Slopes (STRESS-1) studies that span the water column with a vertical spacing of roughly  $5\text{ m}$  prove critical

---

\* Woods Hole Oceanographic Institution Contribution Number 9942.

---

Corresponding author address: Steve Lentz, Woods Hole Oceanographic Institution, Woods Hole, MA 02543.  
E-mail: slentz@whoi.edu

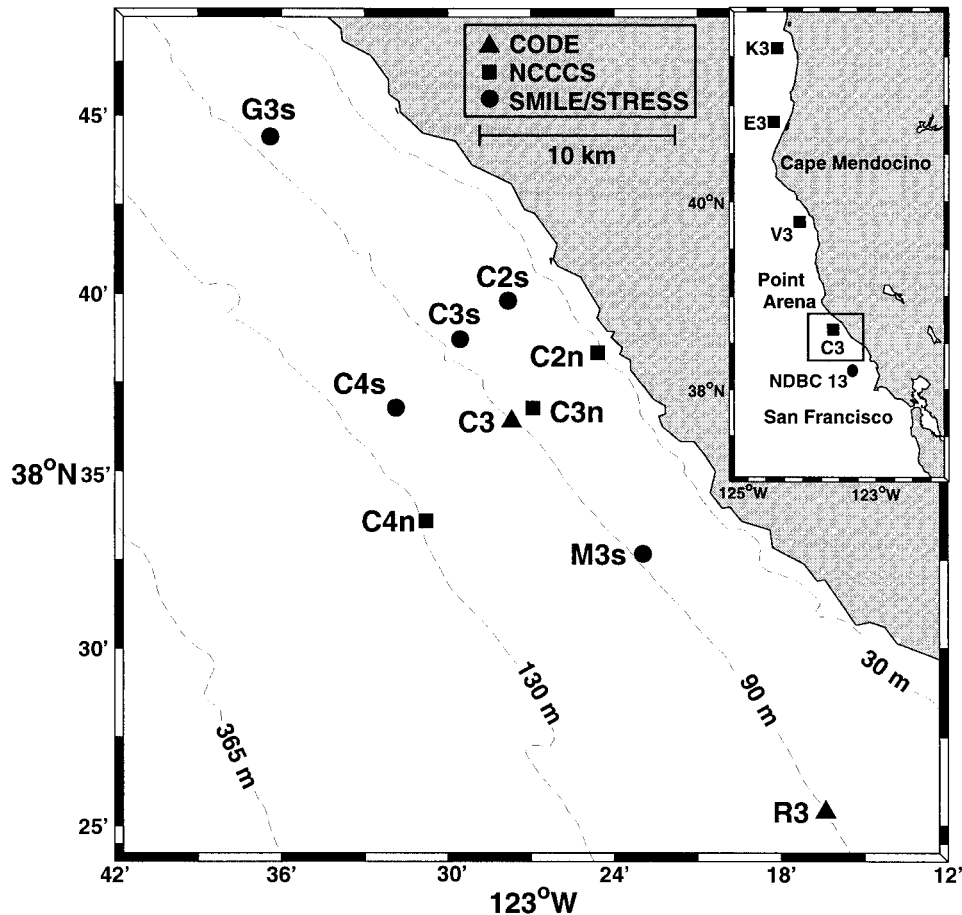


FIG. 1. Map of the northern California shelf showing bathymetry and locations of mooring sites from various field programs. Inset shows locations of NCCCS mooring sites and the NDBC13 wind buoy along the northern California shelf.

in interpreting the mean velocity profiles from other studies at this site with coarser vertical resolution. The dynamics associated with the fall and winter mean flow are examined using ancillary observations during some of the field programs. Of particular interest is whether adjustment of the density field within the bottom boundary layer results in reduced bottom stress.

Of relevance to this study are recent studies of the momentum balances at this site focusing on variability having timescales of days (Dever 1997a; Trowbridge and Lentz 1998). Dever (1997a) uses observations from the SMILE/STRESS study to compare cross-shelf transports in the surface mixed layer, the interior, and the bottom mixed layer to a simple, two-dimensional transport model that neglects density effects. For winter, Dever finds close agreement between the cross-shelf transport in the surface mixed layer and the wind-driven Ekman transport. Most of the cross-shelf return flow is in the interior in both the observations and the model. The cross-shelf transport in the bottom mixed layer is small and there is only moderate agreement between the observed and modeled bottom mixed layer transport.

Trowbridge and Lentz (1998) examine the vertically integrated momentum balances within the bottom mixed layer using the STRESS observations. They find only moderate agreement between the cross-shelf transport anomaly (relative to the interior flow) in the bottom mixed layer and the Ekman transport associated with the bottom stress. In the alongshelf momentum balance they find that the buoyancy force, bottom stress, and Coriolis force are all important. Relative to these two studies, the present study focuses on longer timescales (weeks to months and interannual) and considers data from several other field programs and several other mid-shelf sites.

## 2. Observations

Moored current observations have been acquired at a midshelf site, C3, in approximately 90 m of water off northern California (Fig. 1) during four different field programs in the fall and/or winter of five different years (Table 1). The site was first occupied during the Coastal Ocean Dynamics Experiment (CODE), which included

TABLE 1. Fall and winter time periods when the northern California C3 site was occupied, associated field programs, durations, water depths, and mean wind stresses.

Field program	Time period	Duration (days)	Water depth (m)	$\tau^{xx}$	$\tau^{yy}$
				(10 <sup>-2</sup> N m <sup>-2</sup> )	
CODE	fall 1981 (6 Aug–15 Nov)	101	90	1.5	-4.8
CODE	winter 1981/82 (15 Nov–14 Apr)	150	90	1.2	-1.6
CODE	fall 1982 (21 Aug–15 Nov)	86	90	0.0	-6.0
NCCCS	fall 1988 (1 Aug–15 Nov)	106	90	1.1	-4.8
NCCCS	winter 1988/89 (15 Nov–15 Mar)	120	90	0.4	-3.2
NCCCS	fall 1989 (6 Aug–15 Oct)	70	90	0.9	-6.0*
SMILE/STRESS	winter 1989s (6 Dec–26 Feb)	83	93	-0.4	-3.3
STRESS-II	winter 1990/91 (3 Jan–27 Feb)	56	90	—	—

\* Wind stress record is short.

mooring deployments at C3 during the fall and winter of 1981/82 and the fall of 1982 (Lentz and Chapman 1989). The Northern California Coastal Circulation Study (NCCCS) included a mooring at C3n during the fall and winter of 1988/89 and the fall of 1989 (Largier et al. 1993). The SMILE and STRESS-1 studies during the winter of 1988/89 (Dever 1997a; Trowbridge and Lentz 1998) provide the most well-resolved current profiles at this site (C3s 5 km northwest of the CODE C3 site, Fig. 1), with current meters spaced roughly every 5 m in the vertical over most of the water column. Additionally, a bottom tripod supporting six current meters between 0.5 and 5 m above the bottom was deployed during part of STRESS-1 (Trowbridge and Lentz 1998). (The SMILE/STRESS-1 observations are labeled “winter 1989s” to distinguish them from the winter 1988/89 NCCCS observations.) Current measurements spanning only the lower third of the water column and including bottom tripod measurements were made during the winter of 1990/91 as part of the STRESS-2 field program (Trowbridge and Lentz 1998).

Currents and winds are rotated into a coordinate frame parallel to the local isobaths with the along-isobath direction  $y$  and flow  $v$  positive poleward (toward 317°T for the C3 site), the cross-isobath direction  $x$  and flow  $u$  positive onshore, and  $z$  positive upward. Wind stress  $\tau^s$  is estimated using wind measurements from either the C3 site or a National Data Buoy Center buoy (NDBC 13; inset Fig. 1) and the neutral drag formulation of Large and Pond (1981). Non-neutral wind stress estimates during SMILE are nearly identical to neutral wind stress estimates. Wind stress estimates in the vicinity of the C3 site are well correlated over alongshelf scales of more than 100 km (Dever 1997b). Mean wind stresses for the eight fall and winter periods are weakly equatorward (Table 1), consistent with previous analysis of historical buoy data for this site (Dorman and Winant 1995). Equatorward mean wind stresses are stronger in fall than in winter.

The thermal stratification at the C3 site decreases from fall to winter (Lentz and Chapman 1989; Largier et al. 1993; Dever and Lentz 1994). In fall, the mean vertical temperature gradient is 0.04°C m<sup>-1</sup> in the upper half of

the water column and 0.01°C m<sup>-1</sup> in the lower half of the water column. In winter, the mean vertical temperature gradient is about 0.01°C m<sup>-1</sup> throughout the water column. Density gradients must generally be inferred from temperature because conductivity measurements were not taken. During winter, vertical temperature and density differences from the SMILE/STRESS-1 C3s mooring (which included conductivity sensors) are correlated (correlations between 0.72 and 0.95). Density gradients are estimated from the moored temperature observations assuming a linear relationship between temperature and density with a constant slope of  $b = -0.5$  (kg m<sup>-3</sup>)/°C based on the SMILE/STRESS-1 C3s observations (this value will be used in all subsequent analysis). Brown et al. (1987) found the same average value of  $b$  from moored temperature and conductivity measurements at this site for a 20-day period prior to the 1982 spring transition. Although this value of  $b$  generally estimates density differences with an accuracy of about 20%, during a few events it overestimates density differences by as much as a factor of 2.

Means are calculated over time periods corresponding roughly to fall or winter based on choices made in previous studies or instrument deployment periods. The range of timescales represented by the mean current profiles is examined in section 3.

### 3. Mean current profiles

The fall and winter mean current profiles from the C3 site all have similar vertical structure (Fig. 2). The alongshelf flow is poleward throughout the water column, with a maximum of 5–10 cm s<sup>-1</sup>, often at mid-depth. Mean alongshelf currents are consistently larger in fall than in winter. Year to year (and fall to winter) variations in the mean alongshelf currents are largest in the upper water column. The mean cross-shelf flow is offshore at about 2 cm s<sup>-1</sup> in the upper 20 m of the water column and offshore at about 1 cm s<sup>-1</sup> within 20 m of the bottom. Between the surface and bottom offshore flows there is a 30–40-m thick onshore flow of about 2 cm s<sup>-1</sup>. Both fall to winter and year to year variations in the mean cross-shelf velocities are small.

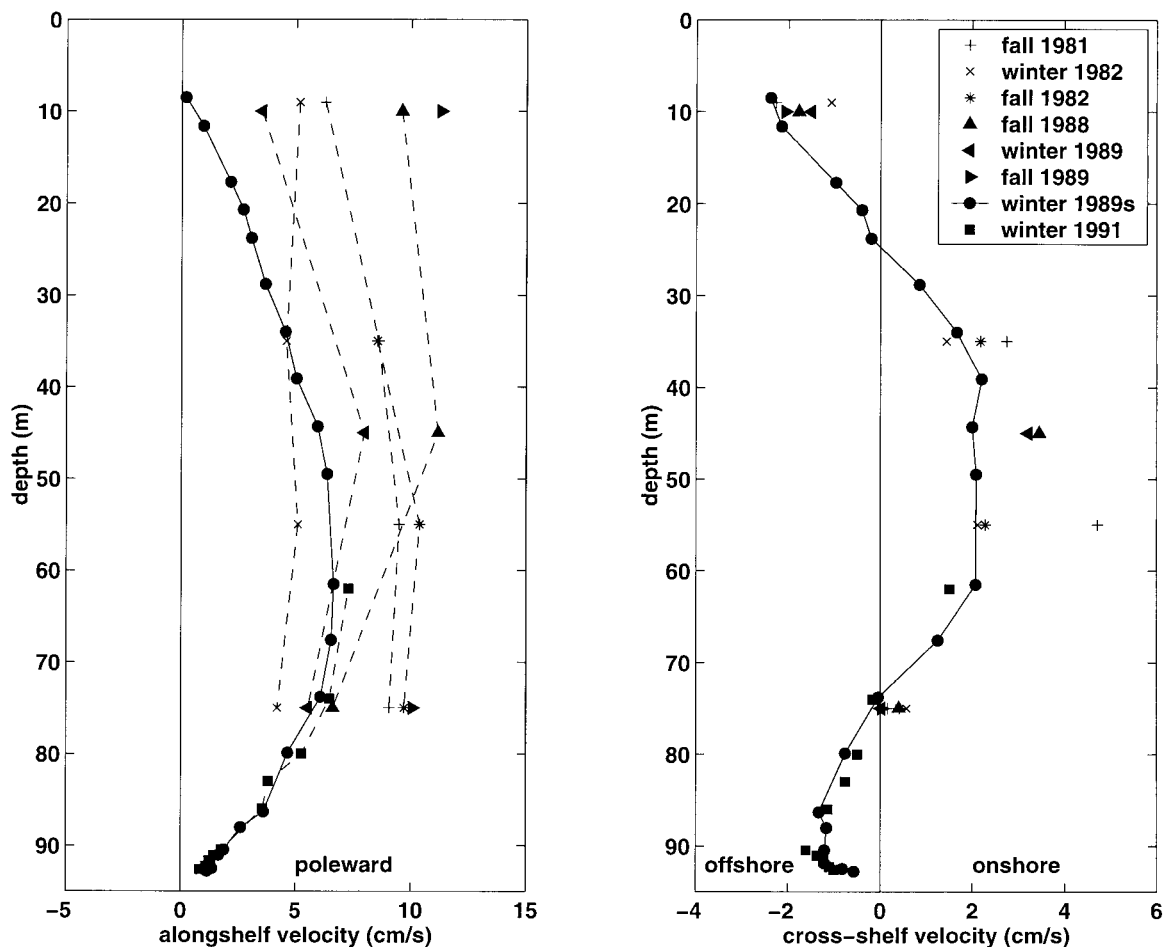


FIG. 2. Mean (left) alongshelf and (right) cross-shelf currents at northern California C3 site as a function of depth for fall and winter of various years. Associated field programs and time periods of means are listed in Table 1. Winter 1990/91 means plotted assuming water depth is 93 m, rather than 90 m, to place near-bottom currents at same elevations as STRESS-1 measurements.

The maximum range at any depth is about  $2 \text{ cm s}^{-1}$  (less near the bottom), much less than the range of the alongshelf mean flows. Note the small range of mean cross-shelf velocities at 15 mab (meters above the bottom) for the eight different deployments. For the winter 1989s mean profile, the interior onshore transport ( $1.9 \text{ m}^2 \text{ s}^{-1}$ ; transports are per unit width) is about equal to the sum of the near-surface ( $1.2 \text{ m}^2 \text{ s}^{-1}$ ) and near-bottom ( $0.6 \text{ m}^2 \text{ s}^{-1}$ ) offshore transports, so the net cross-shelf transport is small (mean, depth-averaged, cross-shelf flow is  $0.1 \text{ cm s}^{-1}$ ).

The mean cross-shelf currents are not large relative to the accuracy of the current meters,  $\sim 2 \text{ cm s}^{-1}$  (Beardsley 1987; Lentz et al. 1995). Temporal averaging or averaging several instruments does not necessarily reduce the error in the current measurements because the uncertainty can be a bias due, for example, to inaccurate averaging of surface waves. The winter 1989s (SMILE/STRESS-1) profile includes three different current meters (vector-measuring current meter, vector-averaging current meter, and benthic acoustic stress sen-

sor) on three different platforms (surface mooring, subsurface mooring, and bottom tripod). The consistency of the vertical structure from these three different measurement techniques and the repeatability of the vertical structure from one experiment to the next (Fig. 2) suggest that the mean profiles are not due to instrument biases. The vertical structure of the mean profiles is not sensitive to the choice of coordinate frames because  $v$  is not much larger than  $u$ . Variations of  $\pm 10^\circ$  in the orientation of alongshelf result in maximum variations of  $\pm 1 \text{ cm s}^{-1}$  in the interior cross-shelf velocity. Changes elsewhere in the water column are smaller for both components of the flow. Standard deviations are about  $10 \text{ cm s}^{-1}$  for the alongshelf currents and  $5 \text{ cm s}^{-1}$  for the cross-shelf currents. Standard errors of the mean are about  $1\text{--}2 \text{ cm s}^{-1}$  for the alongshelf flow and  $1 \text{ cm s}^{-1}$  for the cross-shelf flow. Therefore, fall-to-winter and year-to-year variations in the mean alongshelf velocity profiles are significant in the sense of being much larger than the standard error of the mean. In contrast, vari-

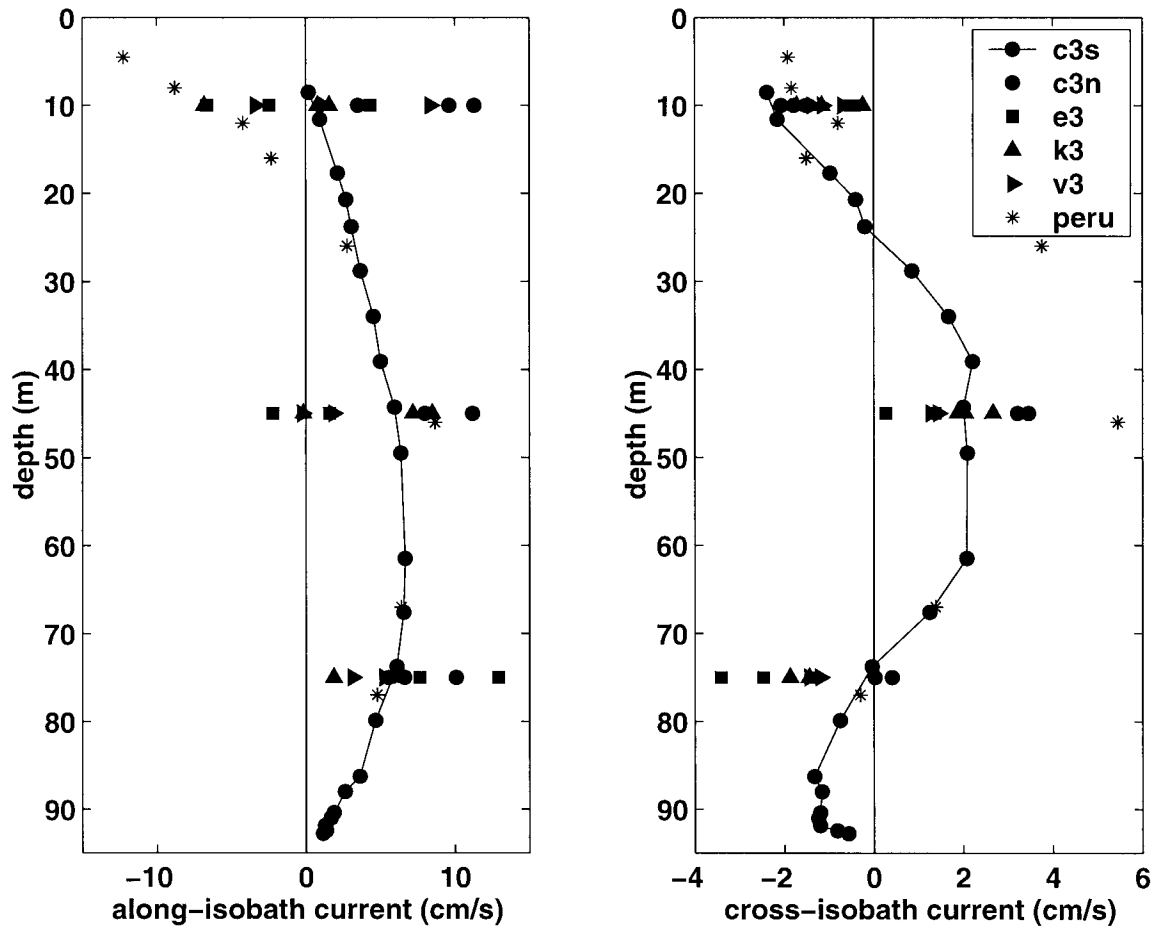


FIG. 3. Mean (left) alongshelf and (right) cross-shelf currents as a function of depth for four midshelf sites along northern California from the NCCCS program and a midshelf site off Peru. For the NCCCS observations there are typically three mean currents plotted for each site, corresponding to fall 1988, winter 1988/89, and fall 1989. The mean current profile for the 1988/89 SMILE/STRESS observations, C3s, is shown for reference.

ations in the mean cross-shelf velocity profiles are generally not significant.

Fall and winter mean current profiles from other sites are similar to those at the northern California C3 site. Mean current profiles (not shown) are similar 30 km south (R3 CODE site) and 8 km offshore (C4s STRESS-2 site) of C3 (Fig. 1). At larger spatial scales, fall and winter mean current profiles from three NCCCS midshelf sites 100 to 300 km north of C3 (K3: 41°35'N, E3: 40°49'N, V3: 39°39'N; Fig. 1) (Largier et al. 1993) have a similar vertical structure (Fig. 3), suggesting that this pattern may be typical along this coast, at least at sites between prominent capes. Mean current profiles from two midshelf sites off Peru (15°S) also show a similar structure (Brink et al. 1980; Smith 1981) (one site, in roughly the same water depth as C3, is shown in Fig. 3).

Mean current profiles during summer are quite different from fall and winter (Winant et al. 1987; Lentz and Chapman 1989; Largier et al. 1993). Summer mean currents are equatorward (5–20  $\text{cm s}^{-1}$ ) and offshore (5

$\text{cm s}^{-1}$ ) in the upper half of the water column, presumably because the mean wind stresses are equatorward, strong, and persistent in summer at this site (Dorman and Winant 1995). In the lower half of the water column, the alongshelf and cross-shelf mean flows are small (1–2  $\text{cm s}^{-1}$ ) during summer.

The consistency of the fall and winter mean profiles suggests that they characterize the average flow on timescales as long as six months. To determine how short a timescale is represented by the fall and winter mean current profiles in Fig. 2, time-average profiles were computed over periods from days to months. Time averages over periods of a week or longer yield profiles similar to those over the interior and lower half of the water column. This is evident in weekly averages of the cross-shelf currents at different depths and from different years (Fig. 4). From August through March weekly averages of the cross-shelf current about 15 mab are confined to a very narrow range,  $\pm 2 \text{ cm s}^{-1}$  (Fig. 4c). Weekly averages 2 mab from the two STRESS studies range between  $-2$  and  $0 \text{ cm s}^{-1}$ . Weekly averages of

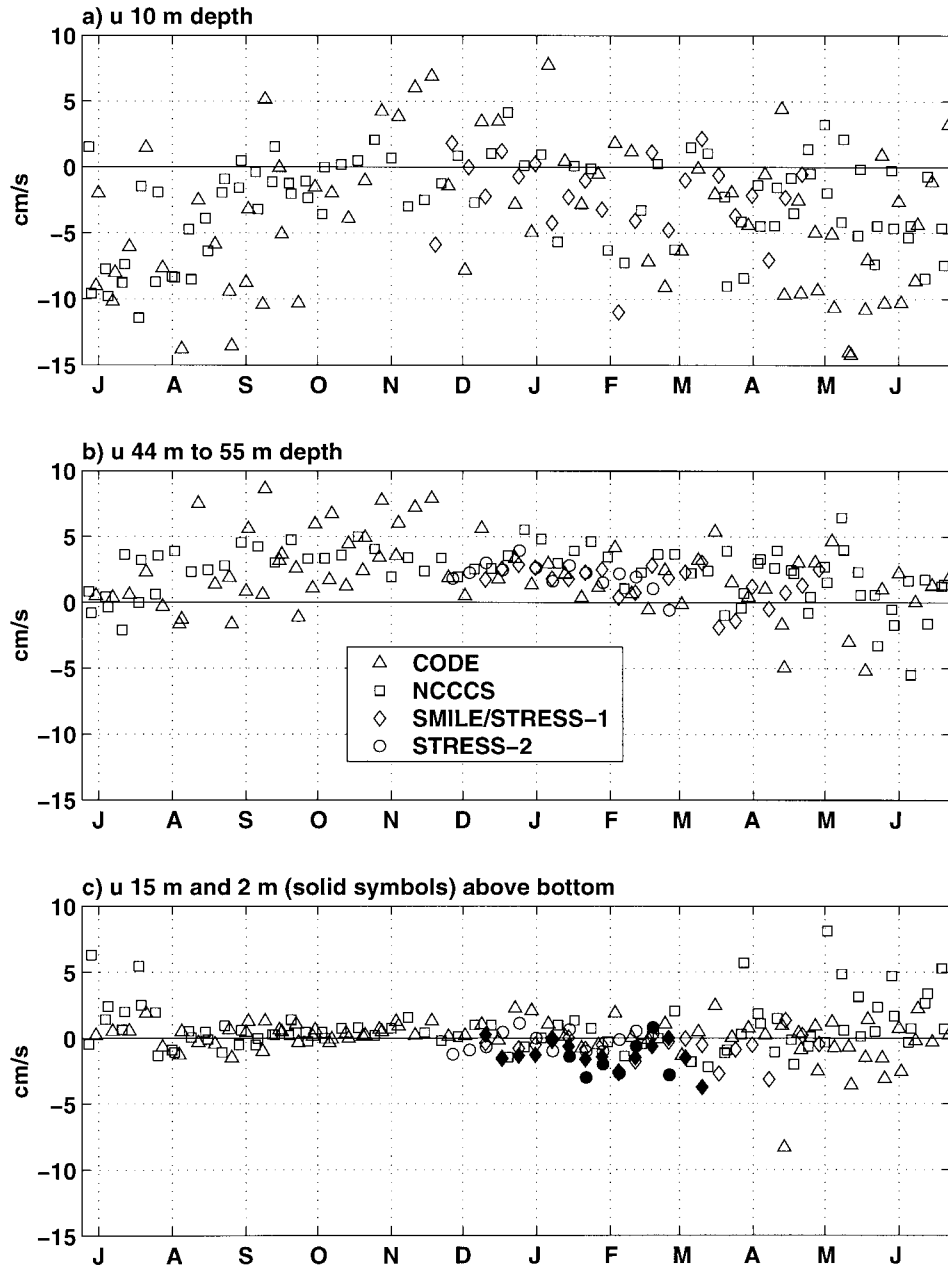


FIG. 4. Weekly averages of cross-shelf currents from the CODE, NCCCS, SMILE/STRESS-1, and STRESS-2 field programs (a) about 10 m below the surface, (b) in the interior, and (c) about 15 and 2 m (solid symbols) above the bottom. The SMILE/STRESS observations overlap in time with the NCCCS observations.

the interior cross-shelf current (Fig. 4b) are almost always positive from August to March, with values typically between 0 and  $5 \text{ cm s}^{-1}$ . In contrast, cross-shelf velocities 10 m below the surface (Fig. 4a) range between  $\pm 10 \text{ cm s}^{-1}$  and averages even over a month are not necessarily offshore as in Fig. 2. Weekly averages of alongshelf currents (not shown) exhibit similar tendencies. Near-bottom and interior alongshelf flows are almost always poleward between 0 and  $20 \text{ cm s}^{-1}$  from

August through March. Near surface flows exhibit a wider range ( $-20$  to  $40 \text{ cm s}^{-1}$ ) and are often equatorward. Thus the basic vertical structure in Fig. 2 does not vary substantially on timescales from weeks to months over the interior and lower part of the water column, but does vary in the upper water column.

The fall and winter mean current profiles may be different during El Niños. In the winter of 1982/83 the mean winter wind stress was poleward ( $0.03 \text{ N m}^{-2}$ )

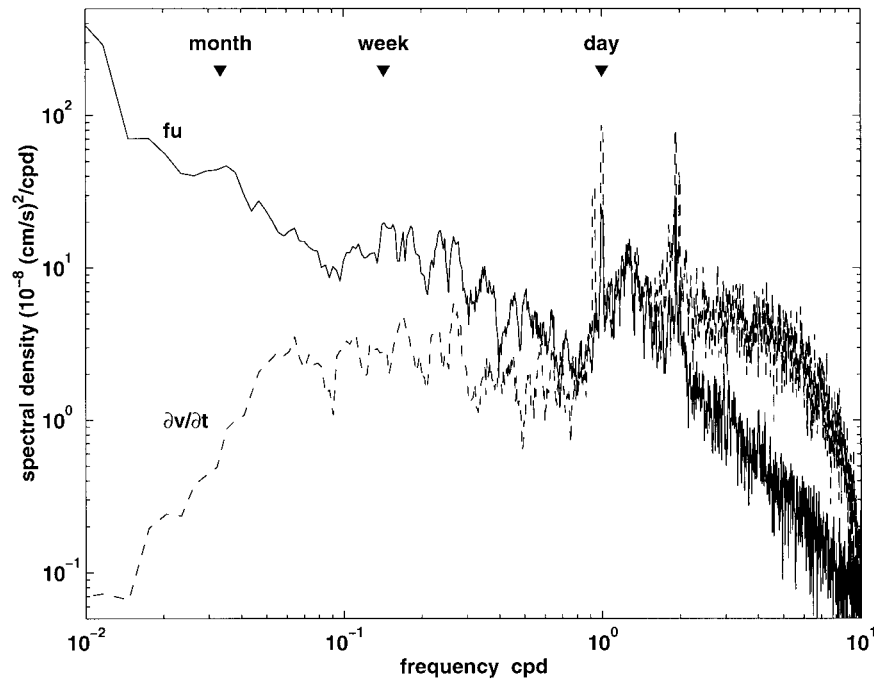


FIG. 5. Spectra of  $\partial v/\partial t$  and  $fu$  at 45-m depth from the NCCCS C3n mooring. The variance in  $fu$  is 6–7 times larger than the variance in  $\partial v/\partial t$  at periods of a week, and more than an order of magnitude larger for periods of a month or longer. Variances of  $\partial u/\partial t$  relative to  $fu$  are even smaller.

rather than equatorward, and the mean current at 10 m depth was poleward, but much larger ( $18 \text{ cm s}^{-1}$ ), and onshore ( $3 \text{ cm s}^{-1}$ ) rather than offshore (Lentz and Chapman 1989). Unfortunately, current observations spanning the water column are not available during the winter of 1982/83 or the fall and winter of 1987/88, which was also an El Niño period (Dorman and Winant 1995).

#### 4. Momentum balances

The dynamical balances associated with the vertical structure of the mean profiles in Fig. 2 are examined in this section. One plausible dynamical interpretation of the mean profiles is that a barotropic alongshelf pressure gradient drives the poleward flow and is opposed by both an equatorward wind stress and a bottom stress (due to the poleward mean flow). In this view, the near-surface and near-bottom offshore transports (relative to the interior) are stress-driven Ekman transports, and the interior onshore flow is in geostrophic balance with the alongshelf pressure gradient. This view is consistent with the two-dimensional transport model used by Dever (1997a) in considering the vertical structure of the current variability on timescales of days. To test portions of this hypothesis, terms in the momentum balances are estimated for timescales of weeks to months using available observations at and near the C3 site.

Temporal accelerations at the C3 site have variances

that are a factor of 6 or more smaller than the Coriolis force for timescales of a week or longer (Fig. 5). Thus for the timescales of interest here, weeks to months, the flow is quasi-steady in the sense that temporal accelerations are small compared to other terms in the momentum balance and may be neglected. The nonlinear advective terms are also neglected because crude estimates from pairs of moorings separated by 5–30 km (Fig. 1) suggest that they are small relative to other terms in the momentum balance. However, uncertainties in both the measurements and resolution of the appropriate spatial scales of gradients in the flow field make the estimates of the nonlinear terms unreliable and hence only suggestive.

We assume both the stress and stress divergence in the interior are small so that the interior cross-isobath ( $u^i$ ) and along-isobath ( $v^i$ ) flow is geostrophic; that is,  $\rho_a f u^i = -\partial P^i/\partial y$  and  $-\rho_a f v^i = -\partial P^i/\partial x$ , where  $\rho_a$  is a reference density,  $f$  is the Coriolis parameter, and  $P^i$  is the interior pressure. This assumption is consistent with the observations that the interior water column remains stratified throughout fall and winter, and coarse Richardson number estimates at middepth from the SMILE moored observations are rarely less than 0.5 (2% of time or less), suggesting that vertical mixing in the interior is small. Pressure measurements to test the assumption of a geostrophic interior are not available. There were two bottom pressure sensors deployed at C2n and C4n during NCCCS, but there were not the necessary interior

temperature or density measurements to determine whether the interior balance was geostrophic (Harms and Winant 1994). Additionally, mean pressure gradients cannot be estimated because of the difficulty in determining the vertical positions of the pressure sensors relative to an absolute reference level (Brown et al. 1987; Harms and Winant 1994). Previous studies have shown that the cross-shelf momentum balance is geostrophic during the summer on timescales of days to weeks (Brink et al. 1980; Brown et al. 1987; Winant et al. 1987), but direct observational evidence that the alongshelf momentum balance is geostrophic in the interior is lacking.

A geostrophic interior and the mean onshore flow in the interior (Fig. 2) imply a poleward, alongshelf pressure gradient. A poleward, alongshelf pressure gradient is also sensible given that the mean wind stress is equatorward (Table 1) and the mean alongshelf flow is poleward during fall and winter (Fig. 2). The depth-averaged alongshelf momentum balance implies a poleward pressure gradient force to balance the wind stress and bottom stress (which act in the same direction), assuming the Coriolis force due to the depth-averaged cross-shelf velocity is small. However, for the reasons noted above direct evidence of an alongshelf pressure gradient is limited (Hickey and Pola 1983; Largier et al. 1993).

In the following two subsections we focus our attention on the dynamical balances associated with the vertical structure of the mean profiles in the upper water column between 0 and 40 m depth and in the lower water column between 60 m depth and the bottom. These depth ranges are based on the mean profiles, particularly the cross-shelf velocity profiles, which indicate stronger vertical shear in these two regions and weaker vertical shear in the interior (discussed above). These two regions are not intended to represent the surface and bottom boundary layer. The boundary layer thickness varies on timescales of days (Lentz and Trowbridge 1991; Lentz 1992) so that a given depth (or height above the bottom) will sometimes be in the boundary layer and sometimes below (or above) the boundary layer. Thus the focus is on whether the observed vertical structure in the mean profiles is primarily associated with geostrophic dynamics, Ekman dynamics, or both. Based on the results in section 3, time series are low-passed filtered to retain variations on timescales of a week or longer.

#### a. Upper water column momentum balances

Assuming hydrostatic flow, subtracting the geostrophic balance at the fixed, interior level  $z^i$  from the momentum balances, and vertically integrating from the surface ( $z = 0$ ) to  $z^i$  yields

$$-fV^s = \frac{\partial B^s}{\partial x} + \frac{\tau^{sx}}{\rho_0}, \quad (1)$$

$$fU^s = \frac{\partial B^s}{\partial y} + \frac{\tau^{sy}}{\rho_0}, \quad (2)$$

where  $(U^s, V^s) = \int_{z^i}^0 (u - u^i, v - v^i) dz$  is the transport anomaly relative to the geostrophic interior velocity and

$$B^s = \int_{z^i}^0 \int_{z^i}^z \frac{g\rho}{\rho_0} dz' dz$$

is the buoyancy anomaly in the upper water column. If the flow in the upper water column is directly wind driven, then the Coriolis force ( $fU^s, fV^s$ ) balances the wind stress, that is, an Ekman balance. If the flow in the upper water column is geostrophic, then the Coriolis force balances the buoyancy gradient and there is an associated thermal wind balance

$$-f \frac{\partial v}{\partial z} = \frac{g}{\rho_0} \frac{\partial \rho}{\partial x}, \quad (3)$$

$$f \frac{\partial u}{\partial z} = \frac{g}{\rho_0} \frac{\partial \rho}{\partial y}. \quad (4)$$

In contrast to (1) and (2), the thermal wind balance provides information about the vertical structure of the momentum balances. When stresses are large, the vertical structure of the momentum balances cannot be determined from the observations because the vertical structure of stress is not known.

For the SMILE observations, transport anomalies relative to the flow at  $z^i = -40$  m are estimated by trapezoidal integration of the eight current time series in the upper 40 m. For the CODE and NCCCS observations there are only two current measurements in the upper 50 m, so transports  $U^s$  and  $V^s$  are estimated assuming the velocity profiles are linear from the surface to  $z^i$  ( $\sim -40$  m). The mean SMILE (winter 1989s) profile (Fig. 2) suggests that assuming a linear profile is reasonable. The correlation between weekly averages of  $fU^s$  and  $\tau^{sy}/\rho_0$  (Fig. 6) is 0.70 for all available fall and winter data (significant at the 99% confidence level for the 96 independent, weekly averages). This supports the assumption that the alongshelf momentum balance in the upper water column is, at least in part, an Ekman balance. However, there is considerable scatter in the comparison and  $fU^s$  is on average about twice  $\tau^{sy}/\rho_0$  (the regression slope is  $2.0 \pm 0.5$ , where the  $\pm$  indicates the 95% confidence interval).

The discrepancies between  $fU^s$  and  $\tau^{sy}/\rho_0$  could be due to inaccuracies in the wind stress or transport estimates. Wind stress estimates from C3 and NDBC-13 are nearly identical, suggesting that the wind measurements are accurate and the scales of the wind field are large (Dever 1997a). Recent comparisons between direct covariance and bulk wind-stress estimates over continental shelves indicate agreement to within 10%–20% (Beardsley et al. 1997; Martin 1998). Thus, the wind stress estimates are probably not the major source of discrepancy between  $fU^s$  and  $\tau^{sy}/\rho_0$ . Uncertainty in the transport estimates could be due to either errors in the current measurements (discussed in section 3) or the assumed vertical structure. A thinner upper layer or a

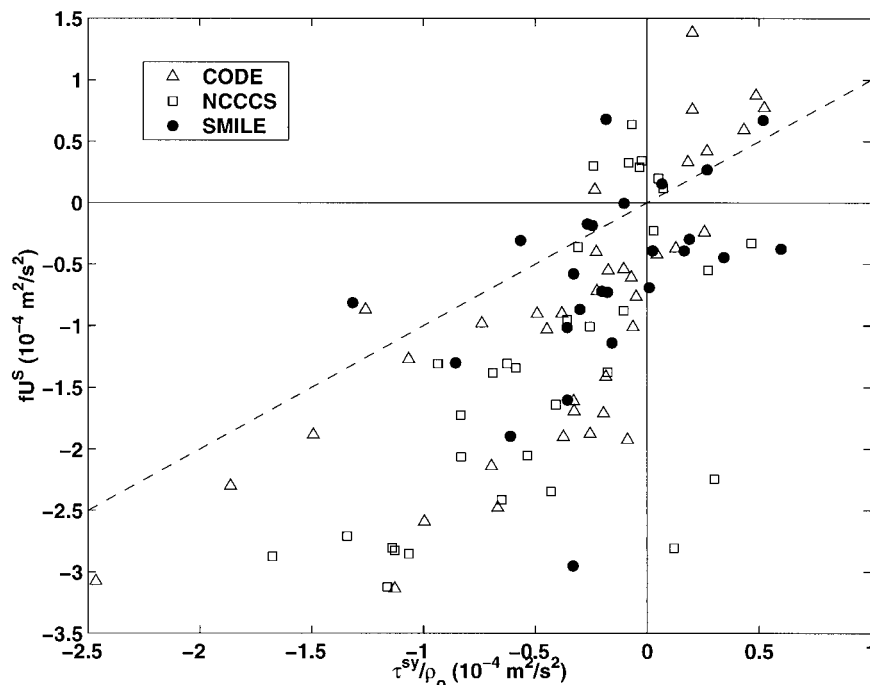


FIG. 6. Comparison of weekly values of terms in surface Ekman balance,  $\tau^{sy}/\rho_o$  and  $fU^s$ , for all available fall and winter data at the C3 site. Correlation is 0.70 and regression slope is 2.0. Dashed line has a slope of one.

near-surface region where the cross-shelf velocity was uniform would reduce the estimate of  $U^s$ . However, simultaneous estimates of  $U^s$  from the C3s SMILE mooring (10 current meters in the upper 50 m) and C3n NCCCS mooring (current meters only at 10 and 45 m) are correlated (0.92) with a regression slope of  $1.2 \pm 0.2$  suggesting poor vertical resolution may not be the major source of the discrepancy between  $fU^s$  and  $\tau^{sy}/\rho_o$ .

Dever (1997a) finds close agreement between the Coriolis force within the surface mixed layer  $fU^{sm1}$  and  $\tau^{sy}/\rho_o$  during SMILE (winter 1988/89) considering timescales longer than a day. To determine whether there is a balance between  $fU^{sm1}$  and  $\tau^{sy}/\rho_o$  at longer timescales, the time series of  $fU^{sm1}$  was low-pass filtered to retain only timescales longer than a week. There is better agreement between  $\tau^{sy}/\rho_o$  and  $fU^{sm1}$  than between  $\tau^{sy}/\rho_o$  and  $fU^s$  (over upper 40 m), correlation 0.86 versus 0.54 and a regression slope of  $0.8 \pm 0.3$  versus  $1.7 \pm 1.6$ . This suggests that much of the discrepancy between  $fU^s$  and  $\tau^{sy}/\rho_o$  is associated with processes extending below the surface mixed layer.

Not surprisingly, the observations suggest discrepancies between  $fU^s$  and  $\tau^{sy}/\rho_o$  may be due to the alongshelf buoyancy gradient  $\partial B^s/\partial y$ . Alongshelf buoyancy gradient estimates from temperature measurements on moorings separated by 5 km (C3s–C3n) or 15 km (C3s–M3) are similar in magnitude to  $fU^s$  and  $\tau^{sy}/\rho_o$  (Figs. 7a and 7b), and the time series of  $\partial B^s/\partial y + \tau^{sy}/\rho_o$  (separation 5 km for  $\partial B^s/\partial y$  estimate) is better correlated with  $fU^s$  than  $\tau^{sy}/\rho_o$  alone (correlation 0.75 vs 0.57,

regression coefficients  $0.78 \pm 0.18$  and  $1.10 \pm 0.15$  respectively; cf. Fig. 7c and 7a). This indicates that the alongshelf density gradient is important in the alongshelf momentum balance within the upper water column at C3 during the winter of 1988/89. In contrast, estimates of  $\partial B^s/\partial y$  from moorings separated by 30 km or more (e.g., SMILE G3s–M3s, CODE C3–R3, NCCCS C3n–V3n) are much smaller, too small to account for differences between  $fU^s$  and  $\tau^{sy}/\rho_o$  in either the mean or fluctuations, and are uncorrelated with  $fU^s - \tau^{sy}/\rho_o$ .

These results suggest that alongshelf buoyancy gradients computed over separations greater than 15 km do not provide accurate estimates for a local balance. The subtidal, near-surface cross-shelf velocities in this region have a correlation scale of about 10 km (Dever 1997b). Dever identifies late January through mid-February and April through early May 1989 as periods when correlation scales of  $u$  near the surface are short and correlations with the wind are reduced at some sites. During these two periods there are large fluctuations in  $\partial B^s/\partial y$  (Fig. 7), suggesting that short correlation scales in cross-shelf velocity are associated with periods of large  $\partial B^s/\partial y$  variability. The alongshelf scale of about 10–15 km is smaller than the separation between major topographic features (Point Reyes, Point Arena, and Cape Mendocino) and is more consistent with mesoscale variability, possibly associated with meandering or instabilities of the alongshelf flow or offshore mesoscale variability impinging on the shelf (Dever 1997b; Largier et al. 1993).

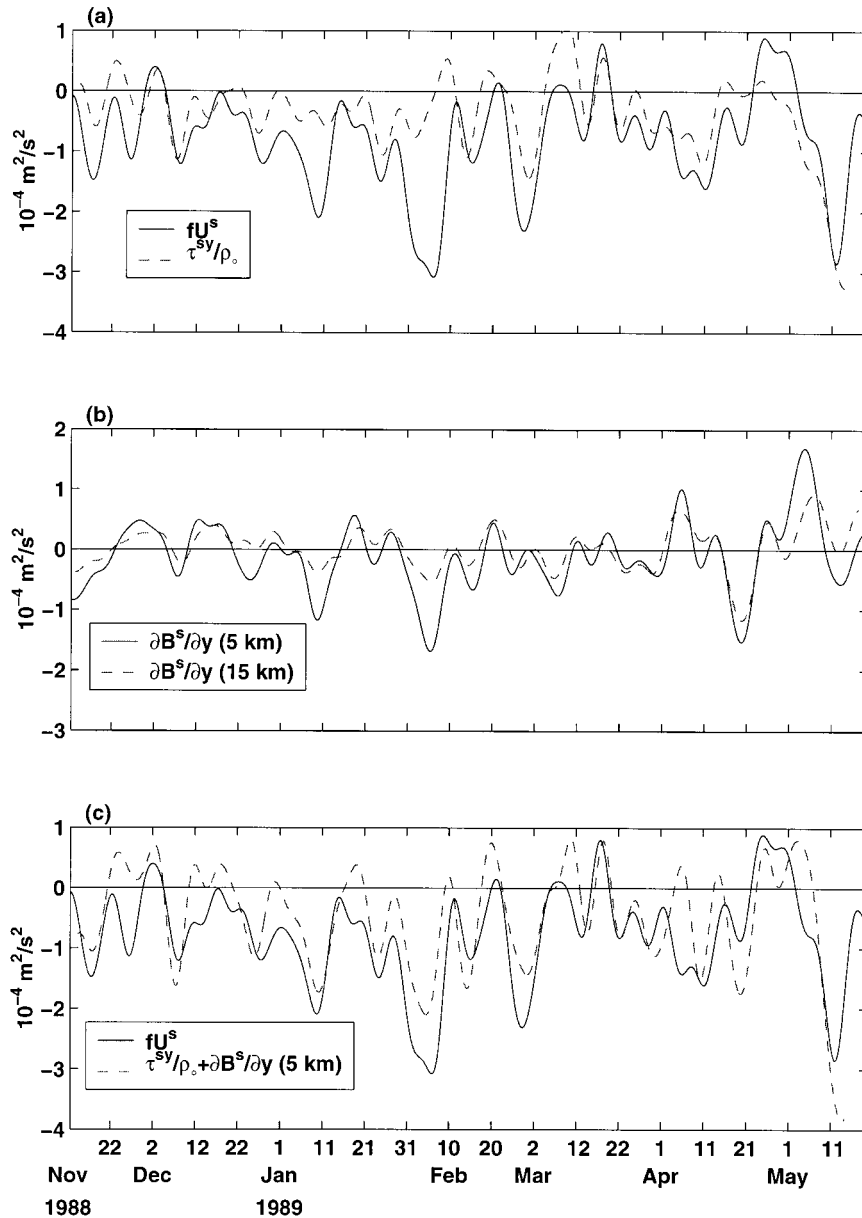


FIG. 7. Time series of terms in alongshelf momentum balance for the upper water column from the SMILE/NCCCS observations: (a)  $fU^s$  and  $\tau^{sy}/\rho_0$  at C3s, (b)  $\partial B^s/\partial y$  from temperature observations at C3s and C3n (separation 5 km) and C3s and M3 (separation 15 km), and (c)  $fU^s$  and  $\tau^{sy}/\rho_0 + \partial B^s/\partial y$  (estimate from C3s and C3n).

The SMILE/STRESS-1 results suggest that alongshelf buoyancy gradients, along with the wind stress, may account for the variability in  $u$  near the surface on timescales of weeks to months (Fig. 4a). The SMILE/NCCCS time series (Fig. 7) and the regression coefficient of 2.0 between  $fU^s$  and  $\tau^{sy}/\rho_0$  (Fig. 6) suggests that  $\partial B^s/\partial y$  is related to the wind stress. The generality of these results remains unclear because accurate estimates of  $\partial B^s/\partial y$  for local balances are not available from the other datasets because the SMILE/STRESS estimates indicate that mooring separations of 15 km or less

are needed. This uncertainty is compounded by the use of temperature to estimate density gradients. There is a clear need for a better characterization and understanding of the density field at these longer timescales.

In contrast to the alongshelf momentum balance, estimates of  $fV^s$  and  $\tau^{sx}/\rho_0$  from the various field programs are uncorrelated (correlation  $-0.03$ ), and  $fV^s$  and  $\partial B^s/\partial x$  are an order of magnitude larger than  $\tau^{sx}/\rho_0$ , indicating that this is not an Ekman balance. Comparisons of either  $fV^s$  and  $\partial B^s/\partial x$  or the terms in the thermal wind balance (3) indicate that the cross-shelf momentum balance is

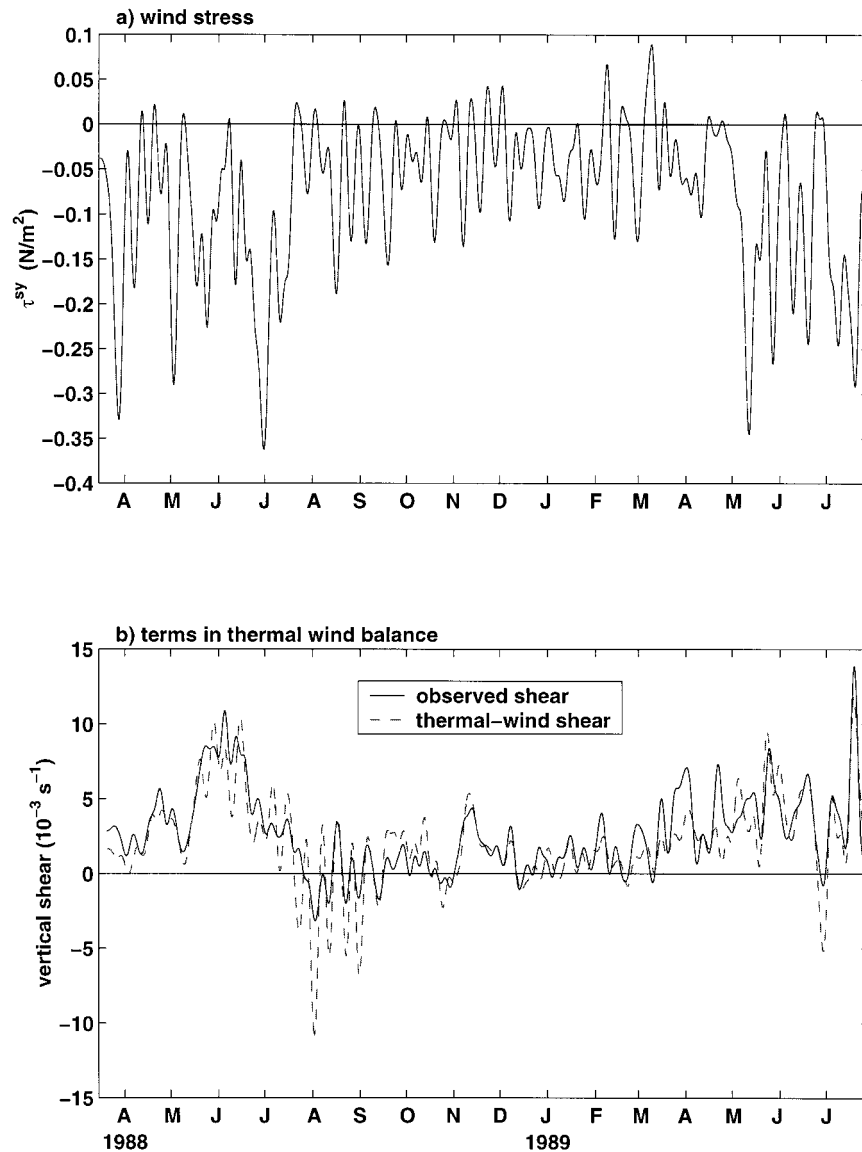


FIG. 8. Time series of (a) alongshelf wind stress and (b) the two terms in the cross-shelf component of the thermal wind balance (3), the observed shear  $\partial v/\partial z$  (estimated at C3n), and the thermal wind shear  $-g(\partial\rho/\partial x)/\rho_0 f$  (estimated from temperature measurements at C2n and C4n) at 10-m depth. Positive thermal wind shears correspond to isopycnals sloping upward toward the coast.

approximately geostrophic during CODE, SMILE, and NCCCS. For example, the vertical shear between 10 and 45 m and the cross-shelf density difference (estimated from temperature) at 10 m from the NCCCS observations are in close agreement (Fig. 8b; correlation 0.84; regression slope  $1.11 \pm 0.03$ ) considering the uncertainty in estimating density from temperature and the potential mismatch in scales between the vertical shear estimate at C3n and the density difference estimate between C2n and C4n (separation 21 km). Differences in the amplitude of the observed shear and the thermal wind shear are probably due in part to seasonal varia-

tions in  $b$  ( $b$ , the constant used to estimate density gradients from temperature gradients, may be smaller, e.g., in the fall of 1988). The discrepancies during the spring of 1989 are probably due to poorly resolved mesoscale variability identified and discussed by both Dever (1997b) and Largier et al. (1993).

The cross-shelf and alongshelf momentum balances in the upper water column provide a qualitatively consistent picture of the low-frequency dynamics in the upper water column. The weak, upwelling-favorable winds drive an offshore Ekman transport in the upper layer that causes the isopycnals to slope upward toward

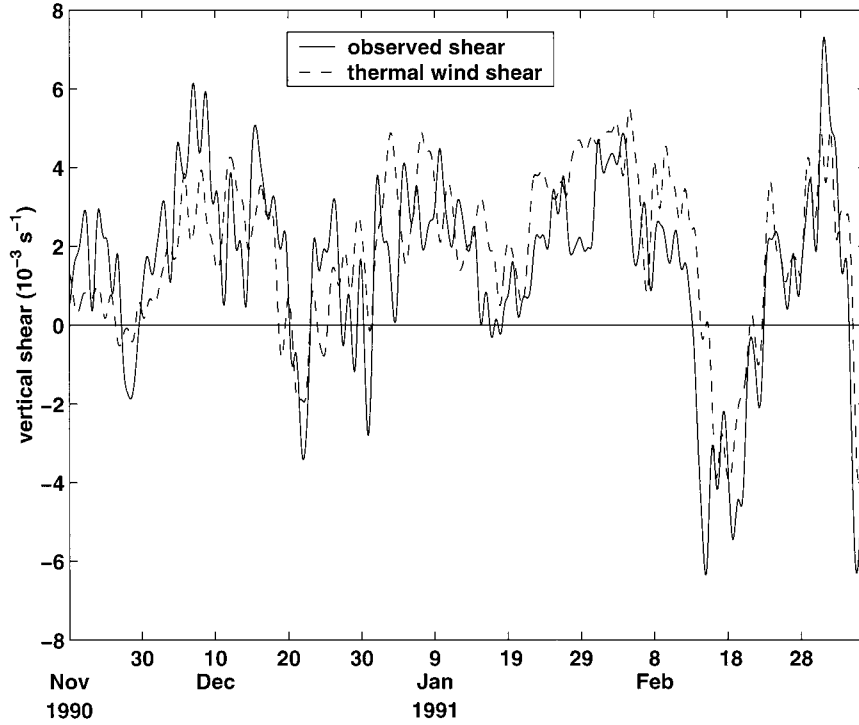


FIG. 9. Time series of the two terms in the cross-shelf component of the thermal wind balance (7), the observed shear  $\partial v/\partial z$  (average of estimates from C3s and C4s), and the thermal wind shear  $-g(\partial\rho/\partial x - \alpha\partial\rho/\partial z)/\rho_0 f$  between C3s and C4s at 19 m above the bottom during STRESS-2. Coordinate frame for estimates is parallel to the bottom. Time series have been low passed with a cutoff period of 33 h.

the coast. The resulting cross-shelf density gradient is in thermal wind balance with the vertical shear in the alongshelf velocity. Thus, both the cross-shelf density gradient and the alongshelf velocity shear depend in part on the strength, duration, and direction of the wind stress, that is, upwelling and downwelling, and on the strength of the stratification. The large positive vertical shears in summer when winds are strongly and persistently upwelling favorable (Fig. 8) is consistent with this scenario. However, other factors, such as alongshelf pressure gradients or mesoscale variability, are probably also important. For example, in August 1988 isopycnals slope downward toward the coast even though the wind stress is weakly upwelling favorable (Fig. 8).

*b. Lower water column momentum balances*

Vertically integrating the momentum balance from the bottom ( $z = 0$ ) to  $z'$  in a new coordinate frame with the  $x$  axis parallel to the bottom and  $z$  perpendicular to the bottom, and making the same assumptions as in section 4a, yields (Trowbridge and Lentz 1998)

$$-fV^b = -\frac{\partial B^b}{\partial x} - g\alpha \int_0^{z_i} (\rho - \rho^i) dz - \frac{\tau^{bx}}{\rho_0}, \quad (5)$$

$$fU^b = -\frac{\partial B^b}{\partial y} - \frac{\tau^{by}}{\rho_0}, \quad (6)$$

where  $(U^b, V^b) = \int_0^{z_i} (u - u^i, v - v^i) dz$  is the near-bottom transport anomaly,  $\alpha = 0.005$  is the bottom slope, and  $(\tau^{bx}, \tau^{by})$  is the bottom stress. The buoyancy anomaly is

$$B^b = \int_0^{z_i} \int_z^{z_i} \frac{g\rho}{\rho_0} dz' dz.$$

The corresponding thermal wind balances are

$$-f\frac{\partial v}{\partial z} = \frac{g}{\rho_0} \left( \frac{\partial \rho}{\partial x} - \alpha \frac{\partial \rho}{\partial z} \right), \quad (7)$$

$$f\frac{\partial u}{\partial z} = \frac{g}{\rho_0} \frac{\partial \rho}{\partial y}. \quad (8)$$

A coordinate frame relative to the bottom is chosen because this is more easily compared with recent theory (Garrett et al. 1993) and because cross-shelf density gradients in this coordinate frame can be directly estimated from subsurface moorings and bottom tripods at sites in different water depths (e.g., C3s and C4s).

The STRESS-1 and STRESS-2 observations provide the best datasets for investigating the momentum balances (5) and (6) in the lower water column. Transport anomalies relative to the interior velocities at  $z_i \approx 30$  mab are estimated by trapezoidal integration using the six to ten current time series in the lower 30 m (Fig.

2). Bottom stresses are estimated using the BASS tripod data and assuming a log profile [see Trowbridge and Lentz (1998) for details]. The alongshelf buoyancy gradient  $\partial B^b/\partial y$  is estimated from the temperature difference between C3n and C3s (separation 5 km) at  $\sim 15$  mab during STRESS-1. Shorter time series of temperature differences from instrument pairs 6 and 18 mab are very similar (correlation 0.94). The cross-shelf buoyancy gradient  $\partial B^b/\partial x$  is estimated from a pair of temperature/conductivity sensors at 19 mab on the STRESS-2 C3s and C4s moorings (separation 8 km). The cross-shelf density difference at 19 mab provides an accurate estimate of the vertical integral because 12 pairs of temperature time series spanning the lower 30 m of the water column and a shorter time series of density at 7 mab indicate that the temperature and density difference between C3s and C4s is vertically uniform over the lower 30 m of the water column on time-scales of days to months.

Focusing first on the cross-shelf momentum balance (5), the transport estimates  $V^b$  at C3s and C4s are similar (correlation 0.75). The bottom stress estimates  $\tau^{bx}$  at C3s and C4s are not correlated but do have similar magnitudes. The Coriolis term  $fV^b$  (average of C3s and C4s) and buoyancy force  $\partial B^b/\partial x + g\alpha \int_0^z (\rho - \rho_i) dz$  are correlated (0.74) and are both about an order of magnitude larger than  $\tau^{bx}/\rho_o$ , indicating that the lower water column cross-shelf momentum balance is approximately geostrophic. Time series of the terms in the thermal wind balance (7) are in close agreement at time-scales longer than a week (correlation 0.82; Fig. 9), indicating that the vertical structure of the along-isobath flow is approximately geostrophic. At timescales shorter than a week, there is less agreement between the terms in the thermal wind balance. (The time series in Fig. 9 have been low passed using a filter with a 33-h cutoff.) The corresponding time-averaged alongshelf velocity profiles from the three STRESS moorings are all roughly linear from 0.3 mab to 10–20 mab, and the slope matches estimates of the mean thermal wind shear [right-hand side of (7)] from the STRESS-2 density measurements at C3s and C4s (Fig. 10). The mean alongshelf velocities near the bottom are weak,  $1 \text{ cm s}^{-1}$  at C3s during both STRESS-1 and STRESS-2 and  $0 \text{ cm s}^{-1}$  at C4s. Recent model studies suggest that for the case of a downwelling favorable (poleward) flow there should be a tendency for a shutdown or reduction of the near-bottom flow and, hence the bottom stress (Trowbridge and Lentz 1991; Garrett et al. 1993; Middleton and Ramsden 1996; Chapman and Lentz 1997). These observations provide evidence for reduction of the near-bottom, along-isobath flow, and hence bottom stress, in a manner consistent with that proposed in these recent model studies. Specifically the models predict a roughly constant vertical shear in the near-bottom along-isobath flow (Fig. 10) that is balanced by a cross-shelf density gradient along the bottom [Eq. (7); Figs. 9 and 10] resulting in a reduction or shutdown of the near-bottom flow (Fig. 10).

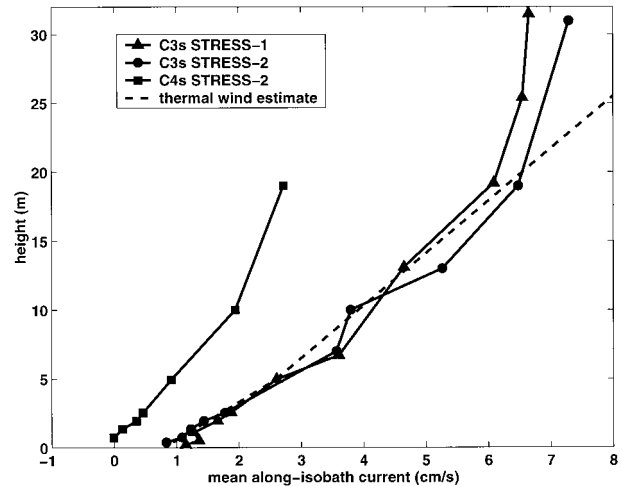


FIG. 10. Observed mean alongshelf velocity profiles at C3s and C4s during STRESS-1 and STRESS-2 and the slope due to the mean cross-shelf density gradient (between C3s and C4s during STRESS-2), assuming a thermal wind balance near the bottom (dashed line). Note that the near-bottom alongshelf velocities are small,  $1 \text{ cm s}^{-1}$  at C3s and  $0 \text{ cm s}^{-1}$  at C4s.

The time series in Fig. 9 suggest a thermal wind balance at timescales of a week or longer, but not at shorter timescales. Spectra of the bottom stress (STRESS-1 and STRESS-2) or near-bottom (15 mab) along-isobath currents (NCCCS and CODE), during fall and winter, reach a maximum at periods between 10 and 50 days and decrease for lower frequencies. There is also a decrease at lower frequencies relative to the interior current (45 mab). While by no means conclusive, these results are consistent with a shutdown time of order 10 days (50 days divided by  $2\pi$ ). An estimate of the shutdown time due to adjustment of the density field within the bottom boundary layer is (Garrett et al. 1993)

$$\frac{1}{2C_D N_i} \left( \frac{f}{\alpha N_i} \right)^3,$$

where  $C_D$  is a bottom drag coefficient and  $N_i$  is the interior buoyancy frequency. Taking  $C_D = 2.5 \times 10^{-3}$  for the interior flow (30 mab) from the log-profile bottom stress estimates (Trowbridge and Lentz 1998), the mean buoyancy frequency of  $N_i = 0.007 \text{ s}^{-1}$  at 37 mab from the density estimates, and  $\alpha = 0.005$  for the bottom slope, yields a shutdown time of about 6 days, in close agreement with the observed timescale. However, the shutdown time is sensitive to  $N_i$  and varies from 1 to 50 days for the range of  $N_i$  observed ( $0.004$ – $0.012 \text{ s}^{-1}$ ).

In the alongshelf momentum balance (6) weekly values of  $fU^b$  and  $-\tau^{by}/\rho_o$  from C3s are correlated during both STRESS-1 (correlation 0.86; Figs. 11a and 12) and STRESS-2 (correlation 0.87). The regression slopes are  $1.1 \pm 0.4$  for STRESS-1 and  $2.1 \pm 1.7$  for STRESS-2. However, in both STRESS-1 and STRESS-2 there are large mean (time average over deployment) transports ( $\sim 0.5 \times 10^{-4} \text{ m}^2 \text{ s}^{-2}$ ) that are not balanced by the mean

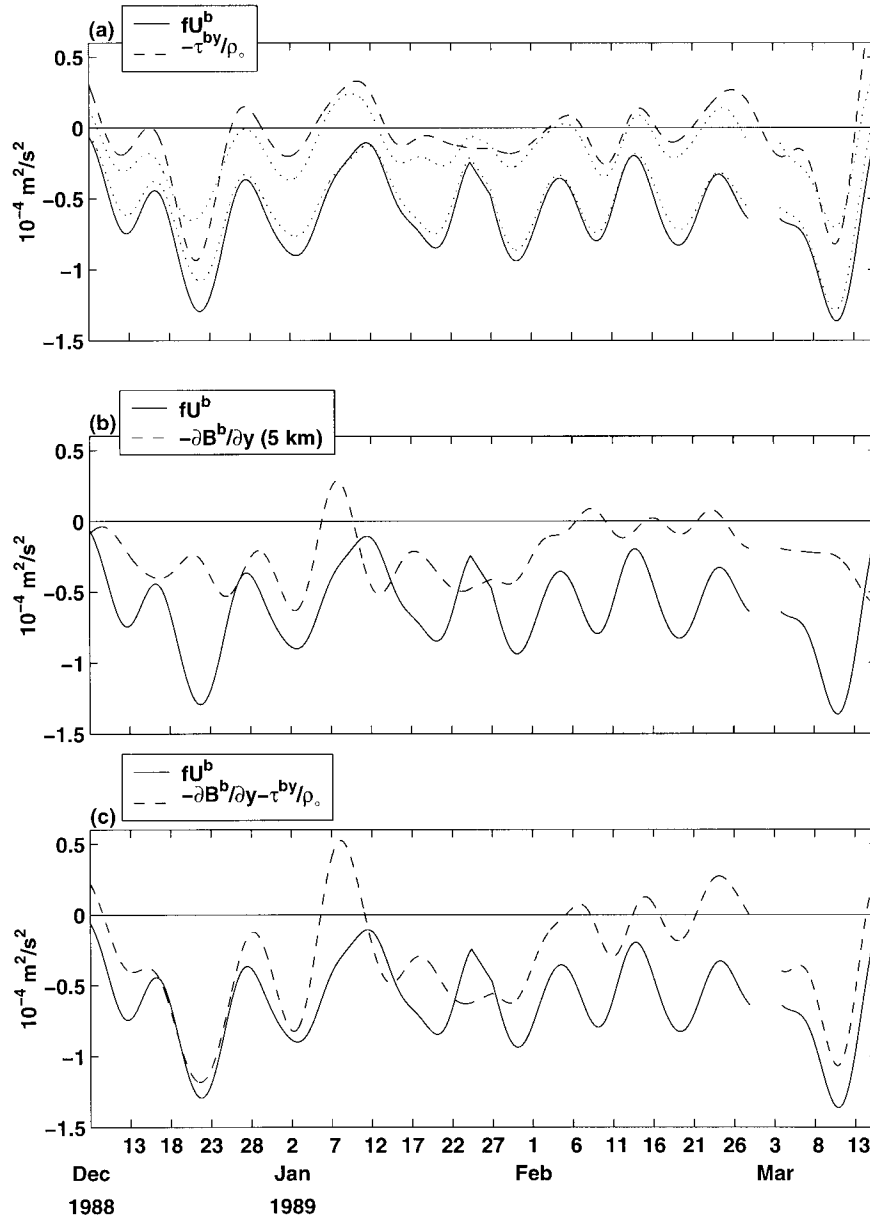


FIG. 11. Time series of terms in the alongshelf momentum balance over the lower water column: (a)  $fU^b$  and  $-\tau^{by}/\rho_o$ , (b)  $fU^b$  and  $-\partial B^b/\partial y$ , and (c)  $fU^b$  and  $-\partial B^b/\partial y - \tau^{by}/\rho_o$ . Estimates of the bottom stress assuming a linear drag law with  $r = 3.4 \times 10^{-4} \text{ m s}^{-1}$  and  $fU^b$  using only observations at 13 and 30 mab are shown for comparison [(a) dotted lines].

bottom stresses (Figs. 11a and 12). Fluctuations in  $\partial B^b/\partial y$  are as large as fluctuations in  $\tau^{by}/\rho_o$  during STRESS-1 (Figs. 11a,b), suggesting that alongshelf buoyancy gradients are significant in the alongshelf momentum balance within the lower water column. The mean  $-\partial B^b/\partial y$  is negative but only partially accounts for the mean  $fU^b$ . Additionally,  $-\partial B^b/\partial y - \tau^{by}/\rho_o$  is not as well correlated with  $fU^b$  (correlation 0.66) as  $\tau^{by}/\rho_o$  alone (Fig. 11c). Uncertainties in  $\partial B^b/\partial y$  are large due to estimating density from temperature, limited in-

formation on the vertical structure of the alongshelf density gradient, and uncertainty in the instrument depths.

Trowbridge and Lentz (1998) find lower correlations between estimates of  $fU^{\text{bml}}$  within the bottom mixed layer and  $-\tau^{by}/\rho_o$  (correlations  $\sim 0.5$ ) during STRESS-1 and STRESS-2. However, the correlations are the same as found here ( $\sim 0.85$ ) if the time series are low-pass filtered to retain only variability at timescales of a week or longer. This indicates that the smaller correlation is due to variability at timescales of days. Trowbridge and

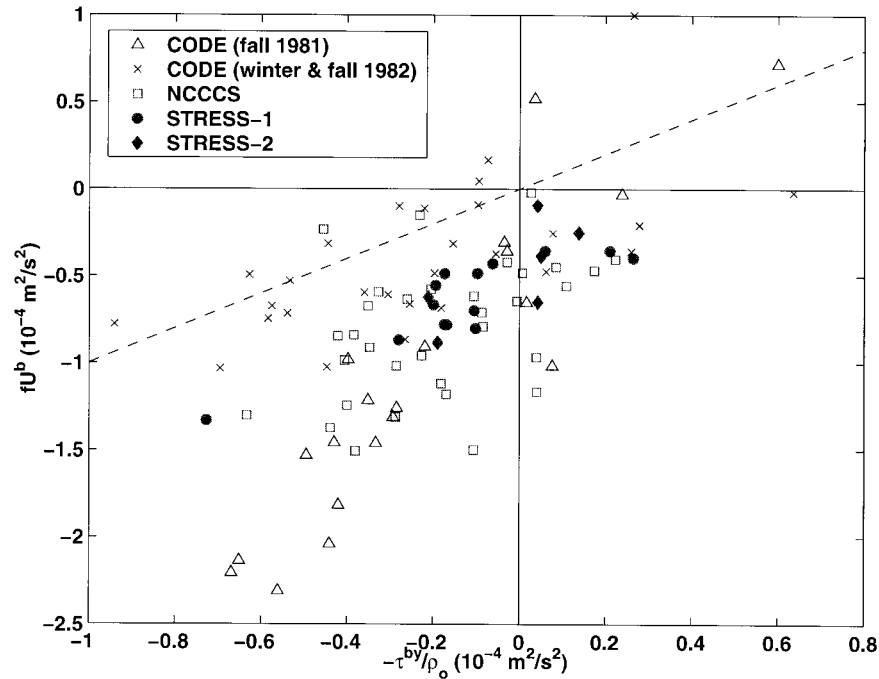


FIG. 12. Comparison of weekly values of terms in the near-bottom Ekman balance,  $fU^b$  and  $-\tau^{by}/\rho_o$ , for all available fall and winter data at the C3 site. Correlation is 0.63, regression slope is 2.2, and intercept is  $-0.3 \text{ m}^2 \text{ s}^{-2}$ . Dashed line has a slope of one.

Lentz (1998) also find that including the buoyancy force  $\partial B^b/\partial y$  (within the bottom mixed layer) does not improve the correlation. However, they find the time-averaged alongshelf momentum balance within the bottom mixed layer closes, in contrast to the large, unbalanced Coriolis force found here. This suggests that the mean Coriolis force is due to the cross-shelf flow above the bottom mixed layer, that is, the steady, onshore flow in the interior. Further evidence for a different set of dynamics in the region above the bottom mixed layer (typically 10–20 m thick) is a comparison of the mean current profiles during upwelling ( $v_i < 0$ ) and downwelling ( $v_i > 0$ ) favorable flows (Fig. 13). Within about 5 m of the bottom, the mean cross-shelf flow is offshore during downwelling and onshore during upwelling. However, from about 10 to 30 mab the mean cross-shelf flow is similar during upwelling and downwelling favorable alongshelf flows. In particular there is a positive mean shear in both cases, suggesting a different set of dynamics from the near-bottom flow.

The STRESS data, and particularly the bottom tripod measurements, are not very long (2–3 months) relative to the timescales of interest. To extend the available data, bottom stresses and cross-shelf transports are estimated using the CODE and NCCCS observations. Bottom stress is estimated using the current measurements at approximately 15 mab and a linear drag law with a linear drag coefficient of  $r = 3.4 \times 10^{-4} \text{ m s}^{-1}$ . This drag coefficient gave the best fit between log-profile estimates of the alongshelf component of bottom stress

and the alongshelf current at 13 mab for weekly averages during the two STRESS studies (correlation 0.83; Fig. 11a, dotted line). Use of a quadratic drag law gives similar results. Cross-isobath transports relative to the interior velocity are estimated from two current measurements, 15 and 35 mab (CODE) or 15 and 45 mab (NCCCS), assuming a vertically uniform interior velocity from 30 to 45 mab, a linearly sloping profile from 30 to 6 mab, and a vertically uniform velocity from 0 to 6 mab, based on the STRESS-1 and STRESS-2 cross-shelf velocity profiles (Fig. 2). The transport estimates are not very sensitive to the details of the assumed vertical structure. For the STRESS observations, assuming this vertical structure and using only the current observations at 13 and 30 mab to estimate transports, yields estimates that are well correlated with the transport estimates using all the current observations (0.89 significant at the 99% confidence level; Fig. 11a, dotted line) with a regression slope of  $0.91 \pm 0.17$ .

Weekly estimates of  $fU^b$  and  $-\tau^{by}/\rho_o$  from all the available data are correlated (0.63; Fig. 12). Linear regression analysis indicates that  $fU^b$  is  $2.2 \pm 0.6$  times larger than  $-\tau^{by}/\rho_o$ , and there is an intercept of  $-0.3 \pm 0.2 \text{ m}^2 \text{ s}^{-2}$ . However, the relationship between  $fU^b$  and  $-\tau^{by}/\rho_o$  appears to be different during the winter of 1981/82 and fall of 1982 ( $\times$  symbols in Fig. 12). Excluding the winter of 1981/82 and fall of 1982 periods, the correlation between  $fU^b$  and  $-\tau^{by}/\rho_o$  is 0.81, the linear regression slope is  $2.4 \pm 0.4$ , and the intercept is  $-0.4 \pm 0.2 \text{ m}^2 \text{ s}^{-2}$ . During the winter of 1981/82 and

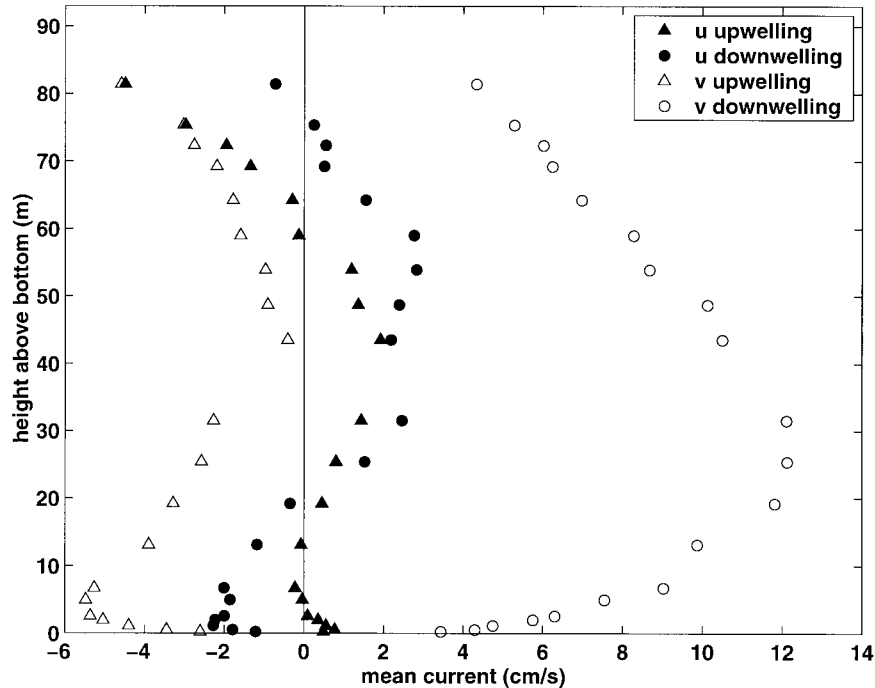


FIG. 13. Time-averaged current profiles during upwelling-favorable ( $v_i < 0$ , triangles) and downwelling-favorable ( $v_i > 0$ , circles) flows from SMILE/STRESS-1 observations. Note the similarity in the cross-shelf velocity profiles between 10 and 30 mab.

fall of 1982 the correlation is 0.70, the slope is  $1.3 \pm 0.6$ , and the intercept is essentially zero ( $-0.1 \pm 0.3 \text{ m}^2 \text{ s}^{-2}$ ). The cause of this difference in the relationship between  $fU^b$  and  $-\tau^{by}/\rho_o$  during the winter of 1981/82 and fall of 1982 is not known. One possibility, suggested by the time series in Fig. 11, is that the alongshelf buoyancy gradient  $\partial B^b/\partial y$  is small during the winter of 1981/82 and fall of 1982 and large at other times. Near-bottom estimates of  $\partial B^b/\partial y$  are only available for STRESS-1 (discussed above) and during CODE. Estimates from the CODE C3 and R3 temperatures (separation 26 km) at 15 mab (again assuming the temperature difference is vertically uniform over the lower layer) are not correlated with the difference between  $fU^b$  and  $-\tau^{by}/\rho_o$  and do not account for the change in the relationship. As observed for the upper water column, the C3 and R3 moorings sites may be too far apart to estimate a local  $\partial B^b/\partial y$  accurately.

The correlation between  $fU^b$  and  $-\tau^{by}/\rho_o$  for the CODE and NCCCS observations should be cautiously interpreted. The bottom stress estimates are proportional to the alongshelf flow and the cross-shelf transport estimates are proportional to the cross-shelf flow, so any dynamics that resulted in veering near the bottom would yield a significant correlation. Nevertheless the available observations suggest that, except during the winter of 1981/82 and fall of 1982, either the bottom stress estimates (from log profiles or a linear drag law) are too small by a factor of 2–3, or some other term in the momentum balance is important. It remains unclear

whether  $\partial B^b/\partial y$  is important because there is very little data available for estimating  $\partial B^b/\partial y$ , the appropriate scales for estimating  $\partial B^b/\partial y$  are not known, and the available data is limited to temperature rather density which may introduce significant uncertainty in the estimates. The limited available data suggest that  $\partial B^b/\partial y$  may be substantial and may account, in part, for the discrepancy between the means of  $fU^b$  and  $-\tau^{by}/\rho_o$  (Fig. 11).

## 5. Summary

Fall and winter mean current profiles for five different years from a midshelf site (water depth  $\sim 90$  m) off northern California exhibit a consistent vertical structure. The alongshelf flow is poleward throughout the water column, with a maximum velocity of 5–10  $\text{cm s}^{-1}$ , often at middepth. There is an offshore flow of about 2  $\text{cm s}^{-1}$  in the upper 20–30 m, an onshore flow of about 2  $\text{cm s}^{-1}$  in the interior (depths 35–65 m), and an offshore flow of about 1  $\text{cm s}^{-1}$  within 20 m of the bottom. A key result of this study is that the mean cross-shelf current profiles do not vary from year to year or from fall to winter (Fig. 2). The mean current profiles are characteristic of timescales from weeks to months (Fig. 4). Similar fall and winter mean current profiles are observed at other midshelf locations along the coast of California and off Peru (Fig. 3).

For timescales of weeks to months, the dynamics are quasi-steady in the sense that accelerations are small

compared to other terms in the momentum balances. The vertical shear in the alongshelf flow is approximately geostrophic throughout the water column, that is, in thermal wind balance with the cross-shelf density gradient (Figs. 8, 9, and 10). Thus periods when the alongshelf flow decreases toward the surface correspond to isopycnals sloping upward toward the coast. This is consistent with the weak, mean upwelling-favorable wind stresses (Table 1) and the corresponding offshore transport in the upper water column (Fig. 2), though other factors also influence the cross-shelf structure of the density field. The decrease in the alongshelf flow toward the bottom corresponds to isopycnals sloping downward toward the coast near the bottom, qualitatively consistent with the offshore flow near the bottom (Fig. 2). The downward sloping isopycnals result in small near-bottom alongshelf currents and bottom stresses. This provides some of the first observational evidence for an adjustment of the flow and density fields near the bottom that results in a reduction of the along-isobath velocity at the bottom, and hence the bottom stress.

The dynamics associated with the vertical structure of the cross-shelf flow are less clear. Offshore transports in the upper and lower water column, relative to the onshore interior flow, are correlated with the surface and bottom stresses. However, in both cases the stresses are generally too small by a factor of about 2 to account for the offshore transports as simple Ekman transports. In the lower water column, there is also a mean (time average over deployment periods) offshore transport that is not balanced by bottom stress (except during the winter of 1981/82 and fall of 1982). Limited data suggests that alongshelf buoyancy gradients, estimated from moorings separated by 5–15 km, in both the upper and lower water column can be substantial and may account for some of the discrepancies between the Coriolis force and the applied stress.

At the beginning of section 4 a simple dynamical interpretation of the mean current profiles was proposed in which a barotropic alongshelf pressure gradient drove a poleward alongshelf flow that was opposed by both the wind stress and the bottom stress, and that the wind stress and bottom stress drove the observed near-surface and near-bottom offshore transports (relative to the geostrophic interior). The observed momentum balances differ from this simple interpretation primarily in the importance of density gradients. The vertical shear in the along-isobath flow is almost entirely balanced by cross-shelf density gradients. The estimated wind stress and bottom stress are not large enough to account for the observed offshore transports (relative to the interior), and limited data suggest that along-isobath density gradients are important. These results suggest that the low-frequency flow is intimately linked to the density field and that a better understanding of the character of the low-frequency density field and the processes that establish that density field are needed.

*Acknowledgments.* We are grateful to the following principal investigators (PI) and their respective groups and co-PIs for acquiring and providing the data used in this study: R. Beardsley, the fall and winter CODE measurements; C. Winant and J. Largier (SIO), the NCCCS measurements; B. Butman (USGS) and S. Williams (WHOI), the STRESS-1 and STRESS-2 measurements; and R. Beardsley (with S. Lentz), the SMILE observations. Comments and suggestions by K. Brink and D. Chapman are appreciated. The manuscript also benefited from suggestions by two anonymous reviewers. S. Lentz was supported by the Office of Naval Research (ONR, N00014-97-1-0161) and J. Trowbridge was supported by National Science Foundation (OCE-9810609) and ONR (N00014-95-0373).

#### REFERENCES

- Beardsley, R. C., 1987: A comparison of the vector-averaging current meter and new Edgerton, Germeshausen, and Grier, Inc., vector-measuring current meter on a surface mooring in CODE 1. *J. Geophys. Res.*, **92**, 1845–1860.
- , A. G. Enriquez, C. A. Friehe, and C. A. Alessi, 1997: Inter-comparison of aircraft and buoy measurements of wind and wind stress during SMILE. *J. Atmos. Oceanic Technol.*, **14**, 969–977.
- Brink, K. H., D. Halpern, and R. L. Smith, 1980: Circulation in the Peruvian upwelling system near 15°S. *J. Geophys. Res.*, **85**, 4036–4048.
- Brown, W. S., J. D. Irish, and C. D. Winant, 1987: A description of subtidal pressure field observations on the northern California shelf during the Coastal Ocean Dynamics Experiment. *J. Geophys. Res.*, **92**, 1605–1636.
- Chapman, D. C., and S. J. Lentz, 1997: Adjustment of stratified flow over a sloping bottom. *J. Phys. Oceanogr.*, **27**, 340–356.
- Csanady, G. T., 1978: The arrested topographic wave. *J. Phys. Oceanogr.*, **8**, 47–62.
- Dever, E. P., 1997a: Wind-forced cross-shelf circulation on the northern California shelf. *J. Phys. Oceanogr.*, **27**, 1566–1580.
- , 1997b: Subtidal velocity correlation scales on the northern California shelf. *J. Geophys. Res.*, **102**, 8555–8571.
- , and S. J. Lentz, 1994: Heat and salt balances over the northern California shelf in winter and spring. *J. Geophys. Res.*, **99**, 16 001–16 017.
- Dorman, C. E., and C. D. Winant, 1995: Buoy observations of the atmosphere along the west coast of the United States, 1981–1990. *J. Geophys. Res.*, **100**, 16 029–16 044.
- Garrett, C., P. MacCready, and P. Rhines, 1993: Boundary mixing and arrested Ekman layers: Rotating stratified flow near a sloping boundary. *Annu. Rev. Fluid Mech.*, **25**, 291–323.
- Harms, S., and C. D. Winant, 1994: Synthetic subsurface pressure derived from bottom pressure and tide gauge observations. *J. Atmos. Oceanic Technol.*, **11**, 1625–1637.
- Hickey, B. M., and N. E. Pola, 1983: The seasonal alongshore pressure gradient on the west coast of the United States. *J. Geophys. Res.*, **88**, 7623–7633.
- Large, W. G., and S. Pond, 1981: Open ocean momentum flux measurements in moderate to strong winds. *J. Phys. Oceanogr.*, **11**, 324–336.
- Largier, J. L., B. A. Magnell, and C. D. Winant, 1993: Subtidal circulation over the northern California shelf. *J. Geophys. Res.*, **98**, 18 147–18 179.
- Lentz, S. J., 1992: The surface boundary layer in coastal upwelling regions. *J. Phys. Oceanogr.*, **22**, 1517–1539.
- , and D. C. Chapman, 1989: Seasonal differences in the current and temperature variability over the northern California shelf

- during the Coastal Ocean Dynamics Experiment. *J. Geophys. Res.*, **94**, 12 571–12 592.
- , and J. H. Trowbridge, 1991: The bottom boundary layer over the northern California shelf. *J. Phys. Oceanogr.*, **21**, 1186–1201.
- , B. Butman, and A. J. Williams III, 1995: Comparison of BASS and VACM current measurements during STRESS. *J. Atmos. Oceanic Technol.*, **12**, 1328–1337.
- Martin, M. J., 1998: An investigation of momentum exchange parameterizations and atmospheric forcing for the Coastal Mixing and Optics program. M.S. thesis, Applied Ocean Physics and Engineering Department, Woods Hole Oceanographic Institution/Massachusetts Institute of Technology, Woods Hole, Massachusetts, 83 pp.
- Middleton, J. F., and D. Ramsden, 1996: The evolution of the bottom boundary layer on the sloping continental shelf: A numerical study. *J. Geophys. Res.*, **101**, 18 061–18 077.
- Smith, R. L., 1981: A comparison of the structure and variability of the flow field in three coastal upwelling regions: Oregon, Northwest Africa, and Peru. *Coastal Upwelling*, F. A. Richards, Ed., Amer. Geophys. Union, 107–118.
- Stahr, F. R., and T. B. Sanford, 1999: Transport and bottom boundary layer observations of the North Atlantic Deep Western Boundary Current at the Blake Outer Ridge. *Deep-Sea Res.*, **46**, 205–243.
- Strub, P. T., J. S. Allen, A. Huyer, R. L. Smith, and R. C. Beardsley, 1987: Seasonal cycles of currents, temperatures, winds, and sea level over the northeast Pacific continental shelf: 35°N to 48°N. *J. Geophys. Res.*, **92**, 1507–1526.
- Trowbridge, J. H., and S. J. Lentz, 1991: Asymmetric behavior of an oceanic boundary layer above a sloping bottom. *J. Phys. Oceanogr.*, **21**, 1171–1185.
- , and ———, 1998: Dynamics of the bottom boundary layer on the northern California shelf. *J. Phys. Oceanogr.*, **28**, 2075–2093.
- Winant, C., R. Beardsley, and R. Davis, 1987: Moored wind, temperature and current observations made during CODE-1 and CODE-2 over the northern California continental shelf and upper slope. *J. Geophys. Res.*, **92**, 1569–1604.